

Mercury(II) Complexes of the Carba-*closo*-dodecaboranyl Ligands [*closo*-1-CB₁₁X₁₁]²⁻ (X = H, F, Cl, Br, I)

Alexander Himmelpach,[†] Jan A. P. Sprenger,[†] Jonas Warneke,^{*,‡} Manfred Zähres,[§] and Maik Finze^{*,†}

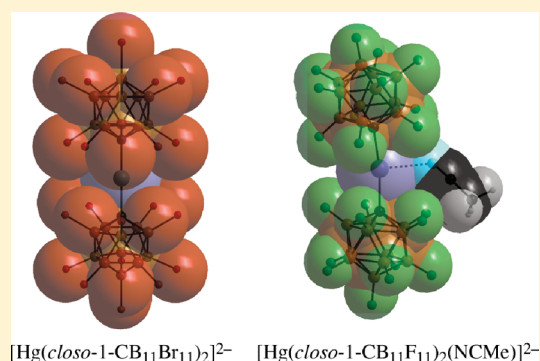
[†]Institut für Anorganische Chemie, Julius-Maximilians-Universität Würzburg, Am Hubland, 97074 Würzburg, Germany

[‡]Institut für Organische Chemie, Fachbereich 2 (Chemie/Biologie), Universität Bremen, Leobener Strasse, NW2, 28359 Bremen, Germany

[§]Institut für Physikalische Chemie, Universität Duisburg-Essen, Universitätsstrasse 5, 45141 Essen, Germany

Supporting Information

ABSTRACT: Salts of the mercury(II) complexes [$\text{Hg}(\textit{closo}\text{-}1\text{-CB}_{11}\text{X}_{11})_2]^{2-}$ (X = H (1), Cl (3), Br (4)) and [$\text{PhHg}(\textit{closo}\text{-}1\text{-CB}_{11}\text{X}_{11})]^-$ (X = H (6), Cl (8), Br (9), I (10)) were synthesized and characterized by multi-NMR spectroscopy, mass spectrometry, elemental analysis, and differential scanning calorimetry. Single crystals of $\text{Cs}_2\cdot 1.2\text{Et}_2\text{O}$, $\text{Cs}_2\cdot 3\cdot \text{MeCN}$, $\text{Cs}_2\cdot 4\cdot 4\text{Me}_2\text{CO}$, Cs_9 , and $[\text{Et}_4\text{N}]^+\cdot 6\cdot 0.5\text{Me}_2\text{CO}$ were studied by X-ray diffraction, and the interpretation of the bond properties is supported by theoretical data. In contrast to the mercury atom of the previously published [$\text{Hg}(\textit{closo}\text{-}1\text{-CB}_{11}\text{F}_{11})_2]^{2-}$ (2), which coordinates either acetonitrile or water, the metal atom of the related dianionic complexes 1, 3, and 4 does not reveal any further coordination. According to results derived from DFT and ab initio calculations, this different behavior is reasoned in the case of 1 by a reduced Lewis acidity at mercury and in the case of 3 and 4 by the increased shielding of the central mercury atom as a result of the bulky halogenated carba-*closo*-dodecaboranyl ligands [$\textit{closo}\text{-}1\text{-CB}_{11}\text{X}_{11}]^{2-}$ (X = Cl, Br). The dianionic complex [$\text{Hg}(\textit{closo}\text{-}1\text{-CB}_{11}\text{I}_{11})_2]^{2-}$ (5) with the bulkiest carba-*closo*-dodecaboranyl ligand was generated via collision-induced dissociation and characterized by (–)-ESI mass spectrometry. The fragmentation pathways of the anionic complexes [$\text{Hg}(\textit{closo}\text{-}1\text{-CB}_{11}\text{X}_{11})_2]^{2-}$ (X = H, F, Cl, Br, I (1–5)) and [$\text{PhHg}(\textit{closo}\text{-}1\text{-CB}_{11}\text{X}_{11})]^-$ (X = H, F, Cl, Br, I (6–10)) were studied by (–)-ESI mass spectrometry.



[$\text{Hg}(\textit{closo}\text{-}1\text{-CB}_{11}\text{Br}_{11})_2]^{2-}$ [$\text{Hg}(\textit{closo}\text{-}1\text{-CB}_{11}\text{F}_{11})_2(\text{NCMe})]^{2-}$

INTRODUCTION

Transition-metal complexes of dicarba-*closo*-dodecaboranyl ligands with an *exo*-polyhedral metal–C_{cluster} σ bond are well-known,^{1,2} and they are used in a number of applications, for example, in catalysis. Important examples are mercury(II) complexes with dicarba-*closo*-dodecaboranyl ligands,^{2–4} which have been investigated with all three isomeric clusters {*closo*-1,2-C₂B₁₀}, {*closo*-1,7-C₂B₁₀}, and {*closo*-1,12-C₂B₁₀}, because they exhibit strong similarities to Hg^{II} complexes with electron-poor perfluoroaryl ligands.^{5,6} Both contain Lewis acidic mercury atoms that can coordinate further neutral as well as anionic ligands and are, therefore, discussed as anion receptors, materials for gas storage, catalysis, or as building blocks in supramolecular chemistry.^{2,4–6}

To the best of our knowledge, only a few related complexes with carba-*closo*-dodecaboranyl ligands and a metal–C_{cluster} σ bond have been described, so far:⁷ [$\text{ClCu}(\textit{closo}\text{-}1\text{-CB}_{11}\text{F}_{11})]^{2-}$,⁸ [$\text{Ag}(\textit{closo}\text{-}1\text{-CB}_{11}\text{I}_5\text{Br}_6)_2]^{3-}$,⁹ and [$\text{PhAu}(\textit{closo}\text{-}1\text{-CB}_{11}\text{H}_{11})]^-$.¹⁰ Recently, we have reported on the tetraethylammonium salts of the mercury(II) complexes [$\text{Hg}(\textit{closo}\text{-}1\text{-CB}_{11}\text{F}_{11})_2]^{2-}$ (2) and [$\text{PhHg}(\textit{closo}\text{-}1\text{-CB}_{11}\text{F}_{11})]^-$ (7) that contain a perfluorinated carba-*closo*-dodecaboranyl ligand.¹¹ Both complexes exhibit high thermal and chemical stability, which is similar to the behavior of the anionic complex [$\text{Ph}_3\text{PAu}(\textit{closo}\text{-}1\text{-}$

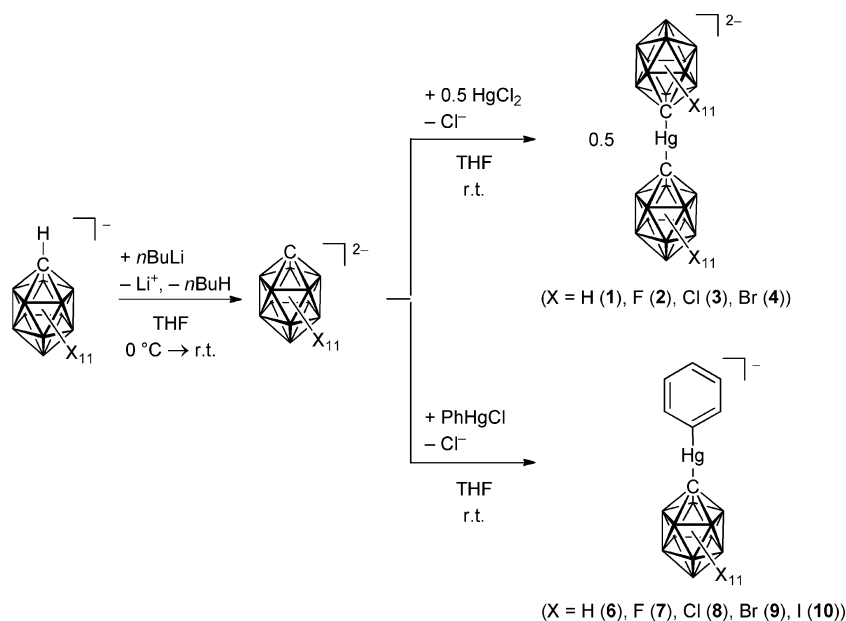
*CB*₁₁H₁₁)][–].¹⁰ In the case of the homoleptic complex 2, the coordination of acetonitrile or water to the Lewis acidic mercury center was observed, and [$\text{Et}_4\text{N}]_2[\text{Hg}(\textit{closo}\text{-}1\text{-CB}_{11}\text{F}_{11})_2(\text{NCMe})]$ ([$\text{Et}_4\text{N}]_2[2\cdot \text{NCMe}]$) and [$\text{Et}_4\text{N}]_4[\text{Hg}(\textit{closo}\text{-}1\text{-CB}_{11}\text{F}_{11})_2(\text{OH}_2)_2]$ ([$\text{Et}_4\text{N}]_4[2_2\cdot \text{OH}_2]$)] were characterized by vibrational spectroscopy and single-crystal X-ray diffraction. Obviously, the fluorinated [*closo*-1-CB₁₁F₁₁]^{2–} ligand results in a similar behavior of Hg^{II} in 2 as found for mercury complexes with perfluoroaryl and dicarba-*closo*-dodecaboranyl ligands. This leads to the question of whether related mercury(II) complexes with carba-*closo*-dodecaboranyl ligands especially with perhalogenated clusters reveal an analogous behavior, or not. We are interested in this topic in connection with our study on the specific characteristics of highly fluorinated {*closo*-1-CB₁₁} clusters in comparison to other halogenated and nonhalogenated {*closo*-1-CB₁₁} derivatives.^{12–14}

Here, we report on the synthesis of the cesium and [$\text{Et}_4\text{N}]^+$ salts of the Hg^{II} complexes [$\text{Hg}(\textit{closo}\text{-}1\text{-CB}_{11}\text{X}_{11})_2]^{2-}$ (X = H

Special Issue: Fluorine in Organometallic Chemistry

Received: October 23, 2011

Published: December 16, 2011

Scheme 1. Synthesis of 1–4 and 6–10 with *n*BuLi as Base

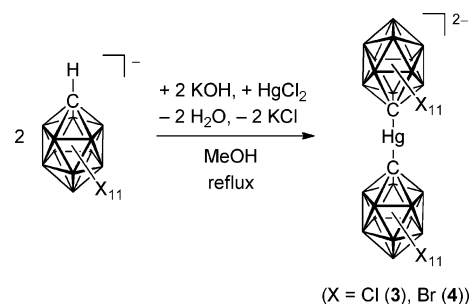
(1), Cl (3), Br (4)) and $[\text{PhHg}(\text{closo-1-CB}_{11}\text{X}_{11})]^-$ (X = H (6), Cl (8), Br (9), I (10)), which were characterized by multi-NMR spectroscopy and elemental analysis. The crystal structures of the cesium salts of all three dianions and of anion 9 as well as of $[\text{Et}_4\text{N}]\text{6}$ were studied by X-ray diffraction, and the discussion of the bond properties is supported by results derived from DFT and ab initio calculations. A possible explanation for the coordination of a further ligand solely to Hg^{II} of the fluorinated derivative 2 and not to its homologues 1, 3, and 4 is provided on the basis of theoretical data. All anions, including the fluorinated complexes $[\text{PhHg}(\text{closo-1-CB}_{11}\text{F}_{11})]^-$ (7) and $[\text{Hg}(\text{closo-1-CB}_{11}\text{F}_{11})_2]^{2-}$ (2) as well as the iodinated derivative $[\text{Hg}(\text{closo-1-CB}_{11}\text{I}_{11})_2]^{2-}$ (5), which was generated in an ion trap, were studied by $(-)$ -ESI mass spectrometry, and the fragmentation patterns of the anions obtained from these Hg^{II} complexes are discussed in detail.

RESULTS AND DISCUSSION

Synthetic Aspects. The dianions $[\text{Hg}(\text{closo-1-CB}_{11}\text{X}_{11})_2]^{2-}$ (X = H, F, Cl, Br (1–4)) are obtained by reactions of mercury dichloride and the dianions $[\text{closo-1-CB}_{11}\text{X}_{11}]^{2-}$, which were synthesized from the corresponding protonated cluster and *n*-butyllithium, as depicted in Scheme 1. The cesium and tetraethylammonium salts are precipitated from aqueous solutions, and in principle, the $[\text{Et}_4\text{N}]^+$ salts can be converted into the Cs^+ salts via an extraction protocol as exemplified for the preparation of $\text{Cs}_2\text{1}$ in the Experimental Section.

For the preparation of salts of 3 and 4, an alternative synthetic route was developed. $\text{Cs}[1\text{-H-closo-1-CB}_{11}\text{X}_{11}]$ (X = Cl, Br) are reacted in situ with HgCl_2 in methanol with KOH as a base (Scheme 2). This method is easier to perform and avoids inert conditions. However, it is not suitable for the synthesis of salts of 1 because $[1\text{-H-closo-1-CB}_{11}\text{H}_{11}]^-$ is not deprotonated in methanol/KOH. Because $\{\text{closo-1-CB}_{11}\text{F}_{11}\}$ clusters undergo partial exchange of the fluorine substituents with hydroxy groups in basic aqueous solution,^{8,13,15} this method seems not to be suited for the preparation of salts of $[\text{Hg}(\text{closo-1-CB}_{11}\text{F}_{11})_2]^{2-}$ (2), as well.

Scheme 2. In Situ Synthesis of 3 and 4



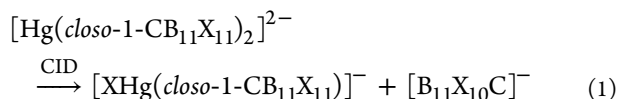
The synthesis of salts of the dianion $[\text{Hg}(\text{closo-1-CB}_{11}\text{I}_{11})_2]^{2-}$ (5) using either route outlined in Schemes 1 and 2 was not successful, so far. The NMR spectroscopic analysis of the reaction mixtures provided some evidence for the formation of products that contain $\text{Hg-C}_{\text{cluster}}$ σ bonds. No cleavage of B–I bonds was observed. These results were confirmed by $(-)$ -ESI as well as $(-)$ -MALDI mass spectrometric studies, and finally the formation of dianion 5 was achieved in an ion trap, as outlined in the following section that describes the mass spectrometric experiments in detail.

The decomposition of the Cs^+ salts of 1–4 starts above 200 °C, as determined by differential scanning calorimetry (DSC). The ^{11}B NMR spectroscopic analysis of the soluble decomposition products in CD_3CN and D_2O showed the formation of the protonated clusters $[1\text{-H-closo-1-CB}_{11}\text{X}_{11}]^-$ (X = H, F, Cl, Br), which is explained by the loss of elemental mercury. However, in an attempt to synthesize the so far unknown dianion $[\text{H}_{11}\text{B}_{11}\text{C-CB}_{11}\text{H}_{11}]^{2-}$, in which both clusters are linked via a carbon–carbon bond, by heating of $\text{Cs}_2\text{1}$ to temperatures ranging from 250 to 400 °C in glass vessels under an Ar atmosphere or in a dynamic vacuum failed, and either unreacted starting material was recovered or insoluble polymeric material was obtained.

The $[\text{Et}_4\text{N}]^+$ and Cs^+ salts of $[\text{PhHg}(\text{closo-1-CB}_{11}\text{X}_{11})]^-$ (X = H, Cl, Br, I (6–10)) are accessible from $[\text{closo-1-CB}_{11}\text{X}_{11}]^{2-}$ and PhHgCl (Scheme 1), similar to the synthesis of salts of the

trianions by (–)-ESI mass spectrometry extends the short list of experimentally observed comparatively small trianions that are stable in the gas phase.¹⁶ Collision-induced dissociation (CID) of these trianions in an ion trap yielded a broad variety of singly and doubly charged anions, including a species that, according to its mass, charge, and isotopic pattern, has the composition $[\text{C}_2\text{B}_{22}\text{HgI}_{22}]^{2-}$, as expected for the dianion **5** (see Figure S5 in the Supporting Information).

The fragmentation reactions of the dianions **1–4** and $[\text{C}_2\text{B}_{22}\text{HgI}_{22}]^{2-}$ were studied by CID in an ion trap, and the fragments were analyzed by (–)-ESI mass spectrometry. For the dianions with the halogen substituents Cl, Br, and I, analogous fragmentation pathways were observed, and the initial reaction is shown in eq 1. In the case of the reaction of **4**, only the fragment $[\text{B}_{11}\text{Br}_{10}\text{C}]^-$ was present in the mass spectrum, whereas $[\text{BrHg}(\text{closo-1-CB}_{11}\text{Br}_{11})]^-$ was not observed. The similar behavior of the dianions **3** and **4** as well as $[\text{C}_2\text{B}_{22}\text{HgI}_{22}]^{2-}$ clearly shows that the latter dianion is $[\text{Hg}(\text{closo-1-CB}_{11}\text{I}_{11})_2]^{2-}$ (**5**).



The ions $[\text{B}_{11}\text{X}_{10}\text{C}]^-$ ($\text{X} = \text{Cl}, \text{Br}, \text{I}$) add water in the ion trap, followed by the loss of HX, to result in $[\text{B}_{11}\text{X}_9\text{OHC}]^-$, as summarized in Scheme 4. Fragmentation of $[\text{XHg}(\text{closo-1-CB}_{11}\text{X}_{11})]^-$ ($\text{X} = \text{Cl}, \text{I}$) proceeds via loss of HgX_2 to result in $[\text{B}_{11}\text{X}_{10}\text{C}]^-$ ($\text{X} = \text{Cl}, \text{I}$). For $[\text{ClHg}(\text{closo-1-CB}_{11}\text{Cl}_{11})]^-$, a competitive reaction via a homolytic cleavage of the Hg–C bond was observed that yields the radical anion $[\text{B}_{11}\text{Cl}_{11}\text{C}]^{\bullet-}$.

$[\text{Hg}(\text{closo-1-CB}_{11}\text{F}_{11})_2]^{2-}$ (**2**) reveals a different behavior. Homolytic Hg–C bond cleavage occurs as the dominant fragmentation reaction (Figure 1). The formation of the radical fragment $[\text{B}_{11}\text{F}_{11}\text{C}]^{\bullet-}$ may be explained by the strong B–F bond, which would have to be broken for the formation of $[\text{B}_{11}\text{F}_{10}\text{C}]^-$. In summary, in the series of mercury(II) complexes with the halogenated ligands **2–5**, formation of $[\text{B}_{11}\text{X}_{11}\text{C}]^{\bullet-}$ is the major fragmentation reaction for $\text{X} = \text{F}$, formation of $[\text{B}_{11}\text{X}_{10}\text{C}]^-$ is the sole reaction found for $\text{X} = \text{Br}$ and I , and both pathways were observed for $\text{X} = \text{Cl}$, although only for the fragmentation of $[\text{ClHg}(\text{closo-1-CB}_{11}\text{Cl}_{11})]^-$. Hence, this parallels the trend in B–Hal bond strengths, which decreases from fluorine to iodine (average bond dissociation energies of the boron trihalides: B–F 613, B–Cl 456, B–Br 357, B–I 260 kJ mol^{-1}).¹⁷ The dianion $[\text{Hg}(\text{closo-1-CB}_{11}\text{H}_{11})_2]^{2-}$ (**1**) undergoes homolytic cleavage of the Hg–C bond similar to **2**.

For the perfluorinated cluster $[\text{B}_{11}\text{F}_{11}\text{C}]^{\bullet-}$, the degradation of the carborate “skeletal structure” occurs, whereas $[\text{B}_{11}\text{Cl}_{11}\text{C}]^{\bullet-}$ does not show any degradation. Again, this might be the consequence of the strong B–F bond and the high stability of small neutral fragments, such as BF_3 . For $[\text{B}_{11}\text{Cl}_{10}\text{C}]^-$, only a single loss of BCl_3 was observed and higher energies were necessary and a much lower intensity of the fragmentation product was found. $[\text{B}_{11}\text{X}_{10}\text{C}]^-$ ($\text{X} = \text{Br}, \text{I}$) do not exhibit any degradation under B–B or B–C bond disruption under the reaction conditions used. The weakness of the B–I bond results in a fragmentation of $[\text{B}_{11}\text{I}_{10}\text{C}]^-$ that only proceeds via loss of iodine and finally yields the radical anion $[\text{B}_{11}\text{IC}]^{\bullet-}$ (see Figure S7 in the Supporting Information). These results show strong parallels to those derived from (–)-ESI mass spectrometric studies on the perhalogenated closo-dodecaborate dianions $[\text{closo-B}_{12}\text{X}_{12}]^{2-}$ ($\text{X} = \text{F}, \text{Cl}, \text{Br}$,

I),¹⁸ and therefore, the presented mercury(II) complexes act in a certain way as a source of the dianions $[\text{closo-CB}_{11}\text{X}_{11}]^{2-}$ that are not accessible from $[\text{1-H-closo-1-CB}_{11}\text{X}_{11}]^-$ under these conditions.¹⁹

The fragmentation patterns of $[\text{PhHg}(\text{closo-1-CB}_{11}\text{X}_{11})]^-$ ($\text{X} = \text{H}, \text{F}, \text{Cl}, \text{Br}, \text{I}$ (**6–10**)) via CID followed by (–)-ESI mass spectrometric analysis are similar to the ones described for the dianions **1–5**. The most important outcome of the study on **6–10** is that, only for $[\text{PhHg}(\text{closo-1-CB}_{11}\text{H}_{11})]^-$ (**6**), a further reaction was found that proceeds via elimination of Hg and formation of $[\text{1-Ph-closo-1-CB}_{11}\text{H}_{11}]^-$ under C–C bond formation (see Figure S8 in the Supporting Information). An analogous reaction was observed for the fragmentation of $[\text{C}_6\text{F}_5\text{Hg}(\text{closo-1-CB}_{11}\text{H}_{11})]^-$, which was formed as a very minor product and could be characterized by mass spectrometry, only. The formation of $[\text{1-C}_6\text{F}_5\text{-closo-1-CB}_{11}\text{H}_{11}]^-$ that also contains the nonhalogenated carba-closo-dodecaboranyl ligand is evident from the (–)-ESI mass spectrum in Figure S1 in the Supporting Information. A similar reaction was not found for the dianionic complex **1**, which is composed of two $[\text{closo-1-CB}_{11}\text{H}_{11}]^{2-}$ parts, probably because of the enhanced Coulomb repulsion of the two dianionic ligands.

Crystal Structure Analysis. $\text{Cs}_2[\text{Hg}(\text{closo-1-CB}_{11}\text{X}_{11})_2]$ ($\text{X} = \text{H}$ (**Cs₂1**), Cl (**Cs₂3**), Br (**Cs₂4**)) crystallize in the centrosymmetric space groups $P2_1/c$ and $P\bar{1}$ as the solvates $\text{Cs}_2\text{1}\cdot 2\text{Et}_2\text{O}$, $\text{Cs}_2\text{3}\cdot \text{MeCN}$, and $\text{Cs}_2\text{4}\cdot 4\text{Me}_2\text{CO}$ (Table 5). The donor atoms of the solvate molecules reveal weak interactions with the cesium cations (see Figures S9–S11 in the Supporting Information). No interaction between these donor atoms and the mercury atoms are present, at all. This observation is in strong contrast to the behavior of the homologous Hg^{II} complex with the fluorinated ligand $[\text{Hg}(\text{closo-1-CB}_{11}\text{F}_{11})_2]^{2-}$ (**2**), which crystallizes with either water or acetonitrile as a further ligand bonded to mercury.¹¹ In all three structures, the mercury atom is located on a center of inversion, resulting in (i) linear C–Hg–C units and (ii) staggered orientations of the carba-closo-dodecaboranyl ligands (Figure 2). The Hg–C

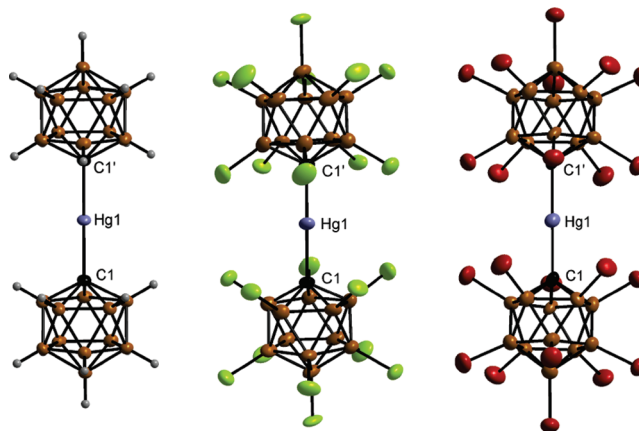


Figure 2. Dianions $[\text{Hg}(\text{closo-1-CB}_{11}\text{X}_{11})_2]^{2-}$ ($\text{X} = \text{H}$ (left, **1**), Cl (middle, **3**), and Br (right, **4**)) in the crystals of $\text{Cs}_2\text{1}\cdot 2\text{Et}_2\text{O}$, $\text{Cs}_2\text{3}\cdot 2\text{MeCN}$, and $\text{Cs}_2\text{4}\cdot 4\text{Me}_2\text{CO}$, respectively (displacement ellipsoids are at the 40% probability level). Selected bond lengths [\AA]: $\text{Cs}_2\text{1}\cdot 2\text{Et}_2\text{O}$, Hg1–C1 2.085(4); $\text{Cs}_2\text{3}\cdot 2\text{MeCN}$, Hg1–C1 2.080(6); $\text{Cs}_2\text{4}\cdot 4\text{Me}_2\text{CO}$, Hg1–C1 2.085(10).

distances of **1**, **3**, and **4** are similar (2.080(6)–2.085(10) \AA) and close to the values determined for $[\text{Et}_4\text{N}]_2[\text{Hg}(\text{closo-1-CB}_{11}\text{F}_{11})_2(\text{NCMe})]$ ($[\text{Et}_4\text{N}]_2[\text{2}\cdot \text{NCMe}]$) and $[\text{Et}_4\text{N}]_4[\{\text{Hg}$

(*closo*-1-CB₁₁F₁₁)₂(OH₂)] ([Et₄N]₄[2·OH₂]) (2.025(17)–2.124(8) Å)¹¹ and mercury(II) complexes with dicarba-*closo*-dodecaboranyl ligands, for example, Hg(12-Ph-*closo*-1,12-C₂B₁₀H₁₀) (2.075 Å).⁴

[Et₄N][PhHg(*closo*-1-CB₁₁H₁₁)]·0.5Me₂CO ([Et₄N]6·0.5Me₂CO) and Cs[PhHg(*closo*-1-CB₁₁Br₁₁)] (Cs9) crystallize in the monoclinic space groups P2₁ and P2₁/c, respectively. The acetone molecule in the structure of [Et₄N]6 does not exhibit any interaction with the two independent anions 6, similar to the dianions 1, 3, and 4 in the structures of their Cs⁺ salts. The Hg–C_{cluster} distances given in Figure 3 are

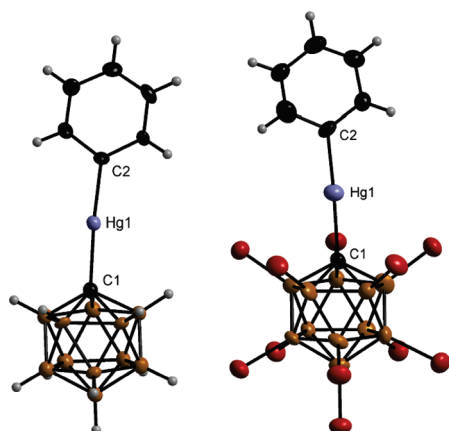


Figure 3. Anions [PhHg(*closo*-1-CB₁₁X₁₁)][−] (X = H (left, 6), Br (right, 9)) in the crystals of [Et₄N]6·0.5Me₂CO and Cs9, respectively (displacement ellipsoids are at the 40% probability level). Selected bond lengths [Å] and angles [deg]: [Et₄N]6·0.5Me₂CO, Hg1–C1 2.082(12), Hg1–C2 2.035(11), C1–Hg1–C2 174.7(5); Cs9, Hg1–C1 2.128(17), Hg1–C2 2.04(2), C1–Hg1–C2 175.9(7).

comparable to those found for 1–4 as well as for [Et₄N]-[PhHg(*closo*-1-CB₁₁F₁₁)] ([Et₄N]7) (2.111(12) Å).¹¹ Slightly shorter *d*(Hg–C) are derived for the mercury–carbon bond with the phenyl ligand, in accordance with the findings reported for [Et₄N]7 (2.062(11) Å). The small deviation from linearity of the C–Hg–C units of the complexes 6 and 9 as well as in 7 (174.2(4) °) is probably a result of packing effects.

The shortest Hg–Br distances of 3.657(2) Å in the dianion 4 and of 3.606(2) Å in the single-negatively charged anion 9, as well as the shortest Hg–Cl distance of 3.514(4) Å in 3, are at the upper limit reported for the sum of the van der Waals radii of mercury (1.70–2.00 Å)²⁰ and bromine (1.85 Å,²¹ in *tert*-alkyl groups) and, respectively, chlorine (1.77 Å,²¹ in *tert*-alkyl groups). Hence, weak interactions between the mercury atoms

and the halogen substituents bonded to the B₅ belt that is connected to the cluster carbon atom cannot be fully excluded. The shortest intercluster Hal–Hal distances in 3 (4.244(4) Å) and 4 (4.198(3) Å) show that there is no significant repulsion between the two ligands coordinated to one mercury atom.

The bonding properties of the mono- and dianionic Hg^{II} complexes calculated using different DFT methods and (RI)-MP2 calculations are in good agreement with the experimental data (selected values are listed in Table S3 in the Supporting Information). At the Slater–Dirac–exchange and the S-VWN level of theory, the structure of [Hg(*closo*-1-CB₁₁I₁₁)₂]^{2−} (5) was calculated, as well. Slightly longer Hg–C bonds are predicted compared to the related mercury(II) complexes, which, in principle, is in agreement with the failure of its synthesis in the condensed phase. However, these differences are rather small, and hence, the failed preparation is more likely due to kinetic effects. This interpretation is supported by the successful generation of dianion 5 via CID, as described in the Mass Spectrometry section.

Coordination of Acetonitrile and Water Solely to [Hg(*closo*-1-CB₁₁F₁₁)₂]^{2−} and Not to [Hg(*closo*-1-CB₁₁X₁₁)₂]^{2−} (X = H, Cl, Br) — A Theoretical Study.

Only for the dianionic complex with the perfluorinated carba-*closo*-dodecaboranyl ligand was the coordination of a further ligand observed, so far.¹¹ It is well documented in the literature that highly fluorinated {*closo*-1-CB₁₁} clusters exhibit a distinct different chemistry compared with those with hydrogen or other halogen substituents.^{7,8,12–14,22} Hence, the unique coordination pattern observed for [Hg(*closo*-1-CB₁₁F₁₁)₂]^{2−} is a further example for such a different behavior.

The coordination to mercury in organomercurials is mostly based on electrostatic interactions,⁵ and so the Lewis acidity of the mercury atom is one of the most important factors that determine the coordination chemistry of such organomercury compounds. A measure for the Lewis acidity of the mercury atoms in [Hg(*closo*-1-CB₁₁X₁₁)₂]^{2−} (X = H, F, Cl, Br, I (1–5)) is, to some degree, the proton affinity of [*closo*-1-CB₁₁X₁₁]^{2−} and the reaction energies for the formations of [Hg(*closo*-1-CB₁₁X₁₁)₂]^{2−} and [PhHg(*closo*-1-CB₁₁X₁₁)][−], which were calculated at different levels of theory (Table 1). For [*closo*-1-CB₁₁H₁₁]^{2−}, the highest proton affinity and the most exothermic reactions are predicted. Hence, this dianion is probably the best electron donor and the mercury atom in 1 should be the least Lewis acidic, which renders the coordination of a third ligand, such as CH₃CN or H₂O, unfavorable. The proton affinities and reaction energies within the series of [*closo*-1-CB₁₁X₁₁]^{2−} dianions (X = halogen) are very similar, and for the fluorinated dianion, the majority of the calculations

Table 1. Calculated Energies of the Reactions of [*closo*-1-CB₁₁X₁₁]^{2−} with H⁺, PhHgCl, and HgCl₂^a

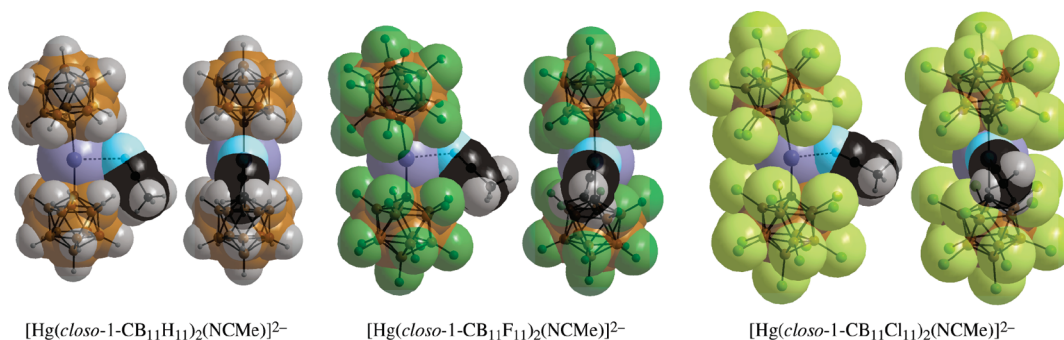
dianion	[<i>closo</i> -1-CB ₁₁ X ₁₁] ^{2−} + H ⁺ → [1-H- <i>closo</i> -1-CB ₁₁ X ₁₁] [−]		[<i>closo</i> -1-CB ₁₁ X ₁₁] ^{2−} + PhHgCl → [PhHg(<i>closo</i> -1-CB ₁₁ X ₁₁)] [−] + Cl [−]			[<i>closo</i> -1-CB ₁₁ X ₁₁] ^{2−} + 0.5HgCl ₂ → 0.5[Hg(<i>closo</i> -1-CB ₁₁ X ₁₁) ₂] ^{2−} + Cl [−]	
	PA ^c	E	E	E	E	E	E
	B3LYP ^b	MP2 ^b	B3LYP ^b	MP2 ^b	SD ^b	MP2 ^b	SD ^b
[<i>closo</i> -1-CB ₁₁ H ₁₁] ^{2−}	1917.2	−1955.5	−426.8	−367.5	−361.1	−318.7	−305.0
[<i>closo</i> -1-CB ₁₁ F ₁₁] ^{2−}	1682.4	−1734.5	−225.6	−185.2	−180.9	−138.3	−129.3
[<i>closo</i> -1-CB ₁₁ Cl ₁₁] ^{2−}	1644.3	−1734.2	−183.2	−212.5	−156.1	−170.2	−105.3
[<i>closo</i> -1-CB ₁₁ Br ₁₁] ^{2−}	1622.6	−1692.0	−161.0	−178.3	−130.7	n.c. ^d	−79.1
[<i>closo</i> -1-CB ₁₁ I ₁₁] ^{2−}	1601.0	−1661.9	−140.4	−153.1	−108.7	n.c. ^d	−50.8

^aAll energies in kJ mol^{−1}. ^bMethods: B3LYP, B3LYP/6-311++G(d,p)/SDD; MP2, (RI)-MP2/def2-SVP/def2-ecp; SD, (RI)-Slater–Dirac/def2-TZVPP/def2-ecp. ^cProton affinity (PA): PA = ΔH_g⁰(base) + ΔH_g⁰(H⁺) − ΔH_g⁰(acid); ΔH_g⁰(H⁺) = 2.5 RT. ^dn.c. = not calculated.

Table 2. Selected Experimental and Calculated Data of $[\text{Hg}(\text{closo-1-CB}_{11}\text{X}_{11})_2(\text{NCMe})]^{2-}$ ($\text{X} = \text{H}$ ($\{1\cdot\text{NCMe}\}$), F ($\{2\cdot\text{NCMe}\}$), Cl ($\{3\cdot\text{NCMe}\}$))^{a,b}

species	method ^a	$d(\text{Hg}-\text{C})$ [Å]	$\angle(\text{C}-\text{Hg}-\text{C})$ [deg]	$d(\text{Hg}\cdots\text{N})$ [Å]	$d(\text{C}\equiv\text{N})$ [Å]	$\angle(\text{Hg}\cdots\text{N}\equiv\text{C})$ [deg]	τ^b [deg]	$\nu(\text{CN})$ [cm^{-1}]	E [kJ mol^{-1}]
{1·NCMe} ^c	MP2	2.074/2.086	175.5	3.081	1.177	122.1	2.8	n.c. ^d	-22.7
	S-VWN	2.064/2.078	175.4	2.983	1.157	119.9	0.4	2310	-19.9
{2·NCMe}	exptl ^e	2.113(14)/ 2.025(17)	167.9(6)	2.689(6)	1.123(10)	145.7(7)	0	2271	n.d. ^f
	MP2	2.082/2.095	172.1	2.770	1.175	133.5	1.9	n.c. ^d	-27.2
	SD	2.108/2.122	171.4	2.699	1.167	132.0	5.1	2255	-15.2
	S-VWN	2.078/2.093	171.3	2.583	1.155	132.3	5.0	2328	-25.6
{3·NCMe}	MP2	2.101/2.109	169.7	2.742	1.174	139.7	25.8	n.c. ^d	5.2
	SD	2.139/2.147	168.9	2.670	1.166	142.9	25.9	2263	10.2
	S-VWN	2.105/2.113	168.6	2.568	1.154	141.6	26.3	2333	4.5
MeCN	exptl ^g				1.157			2254	
	MP2				1.175			n.c. ^d	
	SD				1.168			2251	
	S-VWN				1.156			2324	

^aMethods: MP2, (RI)-MP2/def2-SVP/def2-ecp; SD, (RI)-slater-dirac/def2-TZVPP/def2-ecp; S-VWN, (RI)-S-VWN/def2-TZVPP/def2-ecp. ^b τ = deviation of the carboranyl ligands from an eclipsed conformation (0°). ^cNo minimum for the coordination of acetonitrile to the Hg atom of dianion **1** was found at the (RI)-slater-dirac/def2-TZVPP/def2-ecp level of theory. ^dn.c. = not calculated. ^e $[\text{Et}_4\text{N}]_2[\text{Hg}(\text{closo-1-CB}_{11}\text{F}_{11})_2]$.¹¹ ^fn.d. = not determined. ^gReferences 5 and 23.

**Figure 4.** Representations of the structures of the anionic complexes $[\text{Hg}(\text{closo-1-CB}_{11}\text{X}_{11})_2(\text{NCMe})]^{2-}$ ($\text{X} = \text{H}$ ($\{1\cdot\text{NCMe}\}$), F ($\{2\cdot\text{NCMe}\}$), Cl ($\{3\cdot\text{NCMe}\}$)) calculated at the (RI)-S-VWN/def2-TZVPP level of theory.**Table 3.** Selected Experimental and Calculated Data of $[\text{Hg}(\text{closo-1-CB}_{11}\text{F}_{11})_2(\text{OH}_2)]^{2-}$ ($\{1\cdot\text{OH}_2\}$)

species	method ^a	$d(\text{Hg}-\text{C})$ [Å]	$\angle(\text{C}-\text{Hg}-\text{C})$ [°]	$d(\text{Hg}\cdots\text{O})$ [Å]	τ^b [°]	$\nu_{\text{as}}(\text{OH})$ [cm^{-1}]	$\nu_{\text{s}}(\text{OH})$ [cm^{-1}]	$\delta(\text{HOH})$ [cm^{-1}]	E [kJ mol^{-1}]
{1·OH ₂ }	exptl ^c	2.113(8)/2.087(9)	169.2(3)	2.739(19)	9.1(9)	3681	3583	1587	n.d. ^d
		2.063(9)/2.124(8)	171.3(3)	2.85(2)	2.8(9)				
	MP2	2.089/2.089	173.0	2.666	0.1	n.c. ^e	n.c. ^e	n.c. ^e	-64.0
	SD	2.114/2.115	173.0	2.621	0.4	3506	3420	1500	-53.3
H ₂ O	S-VWN	2.085/2.085	173.2	2.544	0.9	3610	3527	1529	-62.1
	exptl ^f					3756	3657	1595	
	SD					3689	3580	1526	
	S-VWN					3835	3724	1554	

^aMethods: MP2, (RI)-MP2/def2-SVP/def2-ecp; SD, (RI)-slater-dirac/def2-TZVPP/def2-ecp; S-VWN, (RI)-S-VWN/def2-TZVPP/def2-ecp. ^b τ = deviation of the carboranyl ligands from an eclipsed conformation (0°). ^c $[\text{Et}_4\text{N}]_4[\{\text{Hg}(\text{closo-1-CB}_{11}\text{F}_{11})_2\}_2(\text{OH}_2)]$: two different dianions **1** share one aqua. Top row: $\{1\cdot\text{OH}_2\}$ with an occupancy of 70% for H₂O. Bottom row: $\{1\cdot\text{OH}_2\}$ with an occupancy of 30% for H₂O.¹¹ ^dn.d. = not determined. ^en.c. = not calculated. ^fGas phase.²⁴

predict the most exothermic reactions and the highest proton affinity. This is, to some degree, surprising because the electronegativities suggest a different trend. However, these results indicate similar or even higher Lewis acidities for mercury in the higher homologues of $[\text{Hg}(\text{closo-1-CB}_{11}\text{F}_{11})_2]^{2-}$ (**2**) and do not explain the missing coordination of a third ligand to Hg^{II} in $[\text{Hg}(\text{closo-1-CB}_{11}\text{X}_{11})_2]^{2-}$ ($\text{X} = \text{Cl}$ (**3**), Br (**4**)).

In Figure S12 in the Supporting Information, the space-filling models of the calculated structures of $[\text{Hg}(\text{closo-1-CB}_{11}\text{X}_{11})_2]^{2-}$ ($\text{X} = \text{H}, \text{F}, \text{Cl}, \text{Br}, \text{I}$ (**1-5**)) at the (RI)-S-VWN level of theory are depicted. The steric shielding at mercury increases from $\text{X} = \text{H}$ to I , and already for the chlorinated derivative, the central metal atom is effectively shielded, which prevents the interaction with a further ligand. The coordination of acetonitrile to $[\text{Hg}(\text{closo-1-CB}_{11}\text{X}_{11})_2]^{2-}$ ($\text{X} = \text{H}, \text{F}, \text{Cl}$) was modeled by DFT and (RI)-MP2 calculations. The results are

collected in Table 2, and models of the structures are plotted in Figure 4. The bond parameters calculated for $[\text{Hg}(\text{closo-1-CB}_{11}\text{F}_{11})_2(\text{NCMe})]^{2-} \{2 \cdot \text{NCMe}\}$ are in good agreement with experimental values; for example, the calculated structure is very close to an eclipsed conformation as present in the crystal structure. For $\{1 \cdot \text{NCMe}\}$, a very long $d(\text{Hg} \cdots \text{N})$ was calculated, which suggests a weak interaction, only. However, for $\{2 \cdot \text{NCMe}\}$ and $\{3 \cdot \text{NCMe}\}$, similar $d(\text{Hg} \cdots \text{N})$ were predicted, indicating a similar strong coordination. However, for $\{3 \cdot \text{NCMe}\}$, the perchlorinated carba-*closo*-dodecaboranyl ligands are in between a staggered and an eclipsed conformation, showing the increased steric demand of these ligands. In agreement with this observation, coordination of acetonitrile to $[\text{Hg}(\text{closo-1-CB}_{11}\text{Cl}_{11})_2]^{2-}$ (**3**) is not favored, as shown by the calculated energy (Table 2). Hence, the most probable explanation for the nonappearance of the coordination of acetonitrile to **3** and also to **4** is the increased shielding of the central mercury atom rather than an electronic effect.

The coordination of water to **2** was modeled at the different levels of theory used for the study on $2 \cdot \text{NCMe}$, as well (Table 3 and Figure 5). The calculated structures of $2 \cdot \text{OH}_2$ are in close

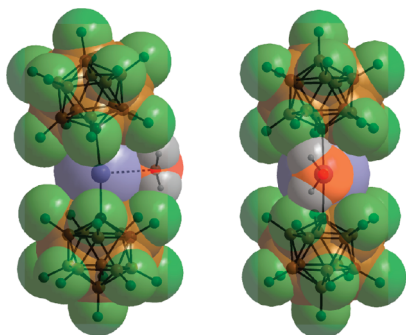


Figure 5. Two representations of the structure of the aqua complex $[\text{Hg}(\text{closo-1-CB}_{11}\text{F}_{11})_2(\text{OH}_2)]^{2-} (2 \cdot \text{OH}_2)$ calculated at the (RI)-S-VWN/def2-TZVPP level of theory.

agreement with those of $[\text{Et}_4\text{N}]_4[\{\text{Hg}(\text{closo-1-CB}_{11}\text{F}_{11})_2\}_2(\text{OH}_2)]$ ($[\text{Et}_4\text{N}]_4[2 \cdot \text{OH}_2]$),¹¹ where two dianions **2** share a single water molecule. The agreement is especially good with the dianion that is bonded to the water molecule with an occupancy of 70%, which has, therefore, a higher percentage of $2 \cdot \text{OH}_2$ than of **2**.

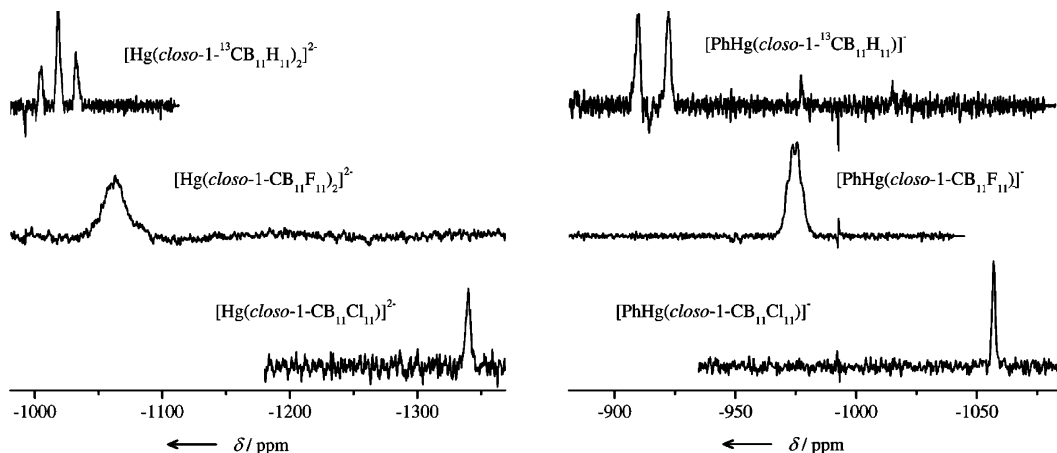


Figure 6. $^{199}\text{Hg}\{^1\text{H}\}$ NMR spectra of $[\text{Hg}(\text{closo-1-CB}_{11}\text{X}_{11})_2]^{2-}$ ($X = \text{H, F, Cl}$ (**1–3**)) and $[\text{PhHg}(\text{closo-1-CB}_{11}\text{X}_{11})]^{2-}$ ($X = \text{H, F, Cl}$ (**6–8**)).

NMR Spectroscopy. The ^{199}Hg chemical shifts of the dianions $[\text{Hg}(\text{closo-1-CB}_{11}\text{X}_{11})_2]^{2-}$ ($X = \text{H, F, Cl, Br}$ (**1–4**)) are found at lower resonance frequencies compared with $\delta(^{199}\text{Hg})$ of the respective anions $[\text{PhHg}(\text{closo-1-CB}_{11}\text{X}_{11})]^{2-}$ ($X = \text{H, F, Cl}$ (**6–10**)), as shown in Figure 6 and listed in Table

Table 4. Selected NMR Spectroscopic Data of $[\text{Hg}(\text{closo-1-CB}_{11}\text{X}_{11})_2]^{2-}$ ($X = \text{H, F, Cl, Br}$ (**1–4**)) and $[\text{PhHg}(\text{closo-1-CB}_{11}\text{H}_{11})]^{2-}$ ($X = \text{H, F, Cl, Br, I}$ (**6–10**))^{a,b}

anion	$\delta(^{199}\text{Hg})$	$\delta(^{13}\text{C})$ C _{cluster}	$\delta(^{13}\text{C})$ C _{phenyl}	$^1J(^{199}\text{Hg}, ^{13}\text{C})$ C _{cluster}	$^1J(^{199}\text{Hg}, ^{13}\text{C})$ C _{phenyl}
1	−1018	81.9		1264	
2^c	−1064	43.3		1702	
3	−1340	80.1		1800	
4	−1311	85.7		1930	
6	−917	87.3	165.8	1139	1332
7^c	−975	47.7	159.4	672	1994
8	−1057	85.2	155.4	936	1837
9	−1002	93.0	155.4	987	1844
10	−865	103.0	148.0	1092	1803

^aSolvent: CD_3CN . ^b δ in ppm and J in Hz. ^cReference 11.

4. Within the two series, a decrease of $\delta(^{199}\text{Hg})$ is observed from the complex with the nonhalogenated cluster to the chlorinated derivative, followed by a small increase starting with the bromine-containing compounds **4** and **9**, and even more for $[\text{PhHg}(\text{closo-1-CB}_{11}\text{I}_{11})]^{2-}$ (**10**) in the series of phenyl complexes.

In comparison to the parent carba-*closo*-dodecaborate anions $[1\text{-H-closo-1-CB}_{11}\text{X}_{11}]^{-7}$ and the related anions $[1\text{-NC-closo-1-CB}_{11}\text{X}_{11}]^{-}$ ($X = \text{H, F, Cl, Br, I}$),¹⁴ the $\delta(^{13}\text{C})$ of the cluster carbon atom is shifted to higher values for **1–4** and even more pronounced for **6–10**. However, the trend in $\delta(^{13}\text{C})$ found within the four analogous series is similar (Table 4).¹⁴ The coupling constants between ^{199}Hg and ^{13}C of the cluster carbon atom are much larger for the homoleptic complexes than for the phenyl derivatives. In the row of the perhalogenated ligands, $^1J(^{199}\text{Hg}, ^{13}\text{C})$ increases from fluorine to the heavier halogen atoms. For $[\text{PhHg}(\text{closo-1-CB}_{11}\text{X}_{11})]^{2-}$ ($X = \text{H, F, Cl}$ (**6–10**)), the increase in $^1J(^{199}\text{Hg}, ^{13}\text{C})$ for the cluster carbon atom is paralleled by a decrease of $^1J(^{199}\text{Hg}, ^{13}\text{C})$ of the *ipso*-carbon atom of the phenyl ligand.

Table 5. Selected Crystal Data and Details of the Refinement of the Crystal Structures of $\text{Cs}_2[\text{Hg}(\text{closo-1-CB}_{11}\text{H}_{11})_2]\cdot 2\text{Et}_2\text{O}$ ($\text{Cs}_2\mathbf{1}\cdot 2\text{Et}_2\text{O}$), $\text{Cs}_2[\text{Hg}(\text{closo-1-CB}_{11}\text{Cl}_{11})_2]\cdot \text{MeCN}$ ($\text{Cs}_2\mathbf{3}\cdot \text{MeCN}$), $\text{Cs}_2[\text{Hg}(\text{closo-1-CB}_{11}\text{Br}_{11})_2]\cdot 4\text{Me}_2\text{CO}$ ($\text{Cs}_2\mathbf{4}\cdot 4\text{Me}_2\text{CO}$), $[\text{Et}_4\text{N}][\text{PhHg}(\text{closo-1-CB}_{11}\text{H}_{11})_2]\cdot 0.5\text{Me}_2\text{CO}$ ($[\text{Et}_4\text{N}]\mathbf{6}\cdot 0.5\text{Me}_2\text{CO}$), and $\text{Cs}[\text{PhHg}(\text{closo-1-CB}_{11}\text{Br}_{11})_2]$ ($\text{Cs}\mathbf{9}$)

	$\text{Cs}_2\mathbf{1}\cdot 2\text{Et}_2\text{O}$	$\text{Cs}_2\mathbf{3}\cdot \text{MeCN}$	$\text{Cs}_2\mathbf{4}\cdot 4\text{Me}_2\text{CO}$	$[\text{Et}_4\text{N}]\mathbf{6}\cdot 0.5\text{Me}_2\text{CO}$	$\text{Cs}\mathbf{9}$
empirical formula	$\text{C}_{10}\text{H}_{42}\text{B}_{22}\text{Cs}_2\text{HgO}_2$	$\text{C}_4\text{H}_3\text{B}_{22}\text{Cl}_{22}\text{Cs}_2\text{HgN}$	$\text{C}_{14}\text{H}_{24}\text{B}_{22}\text{Br}_{22}\text{Cs}_2\text{HgO}_4$	$\text{C}_{33}\text{H}_7\text{B}_{22}\text{Hg}_2\text{N}_2\text{O}$	$\text{C}_7\text{H}_5\text{B}_{11}\text{Br}_{11}\text{CsHg}$
formula wt	898.67	1549.20	2718.58	1157.97	1420.53
T (K)	173	173	290	295	290
cryst syst	monoclinic	triclinic	triclinic	monoclinic	monoclinic
space group	$P2_1/c$	$P\bar{1}$	$P\bar{1}$	$P2_1$	$P2_1/c$
a (Å)	13.1322(8)	9.145(2)	11.853(2)	10.908(2)	15.261(3)
b (Å)	11.4190(5)	9.439(2)	12.584(3)	17.524(4)	9.556(2)
c (Å)	11.7541(6)	14.881(3)	12.958(3)	13.362(3)	20.195(4)
α (deg)		79.62(3)	70.20(4)		
β (deg)	115.264(7)	73.49(3)	66.00(3)	101.36(3)	108.83(3)
γ (deg)		66.73(3)	65.59(3)		
volume (Å ³)	1594.01(17)	1128.0(4)	1573.7(8)	2504.2(9)	2787.5(10)
Z	2	1	1	2	4
D_{calcd} (mg m ⁻³)	1.872	2.281	2.869	1.536	3.385
μ (mm ⁻¹)	7.090	6.320	17.577	6.153	22.577
F(000)	836	708	1210	1136	2488
no. of collected reflns	9157	9681	13 939	25 896	22 790
no. of unique reflns, R(int)	2798, 0.029	3930, 0.050	5478, 0.048	7392, 0.050	5998, 0.128
no. of parameters/restraints	226/68	244/3	299/0	551/145	280/30
R1 ($I > 2\sigma(I)$)	0.019	0.042	0.044	0.037	0.082
wR2 (all)	0.040	0.128	0.119	0.118	0.198
GOF on F ²	1.044	1.127	1.045	1.082	1.190
largest diff. peak/hole (e Å ⁻³)	0.796/−0.841	1.420/−2.041	1.753/−1.472	1.888/−1.794	1.534/−2.771
CCDC no.	847883	847882	847881	847885	847884

SUMMARY AND CONCLUSION

The homoleptic mercury(II) complexes of carba-*closo*-dodecaboranyl ligands $[\text{Hg}(\text{closo-1-CB}_{11}\text{X}_{11})_2]^{2-}$ (X = H, F, Cl, Br (**1–5**)) are easily accessible. As a result of the high steric demand of the $[\text{closo-1-CB}_{11}\text{I}_{11}]^{2-}$ ligand, the coordination of two of these ligands to mercury(II) failed in the condensed phase. However, in principle, two of these bulky ligands can bind to one mercury center, as proven by collision-induced fragmentation reactions starting from trianions containing three $\{\text{Hg}(\text{closo-1-CB}_{11}\text{I}_{11})\}$ segments, which resulted in the formation of $[\text{Hg}(\text{closo-1-CB}_{11}\text{I}_{11})_2]^{2-}$ (**5**) in the gas phase. The synthesis of phenylmercury complexes with one $[\text{closo-1-CB}_{11}\text{X}_{11}]^{2-}$ ligand $[\text{PhHg}(\text{closo-1-CB}_{11}\text{X}_{11})]^-$ (X = H, F, Cl, Br, I (**6–10**)) is straightforward, whereas for the attempted synthesis of $[\text{C}_6\text{F}_5\text{Hg}(\text{closo-1-CB}_{11}\text{X}_{11})]^-$ (X = H, F, Cl, Br, I), dismutation was observed to result in $[\text{Hg}(\text{closo-1-CB}_{11}\text{X}_{11})_2]^{2-}$ and $\text{Hg}(\text{C}_6\text{F}_5)_2$.

Only for $[\text{Hg}(\text{closo-1-CB}_{11}\text{F}_{11})_2]^{2-}$ (**2**) was the coordination of a third, neutral ligand to mercury observed,¹¹ whereas for its higher homologues **3** and **4** and the nonhalogenated anion **1**, no additional coordination was found. In the case of dianion **1**, the reduced Lewis acidity of the mercury atom is most likely the reason for the different behavior. In contrast, for the chlorinated and brominated derivatives **3** and **4**, the Lewis acidity of mercury is probably similar or slightly higher compared to that of the mercury center in **2**. The increased steric demand of the ligands as a result of the larger halogen substituents prevents in the case of **3** and **4** the interaction with a further ligand.

Because of their high thermal and chemical stability, the dianionic homoleptic complexes with the perhalogenated ligands $[\text{Hg}(\text{closo-1-CB}_{11}\text{X}_{11})_2]^{2-}$ (X = F, Cl, Br (**2–4**)) may serve as weakly coordinating dianions similar to halogenated

closo-dodecaborate dianions.²⁵ Furthermore, mercury complexes of this type with carba-*closo*-dodecaboranyl ligands that have functional groups bonded to the cluster boron atoms, for example, alkynyl substituents, are potential building blocks for coordination polymers and supramolecular chemistry.

EXPERIMENTAL SECTION

General Methods. ¹H, ¹¹B, ¹³C, ¹⁹F, and ¹⁹⁹Hg NMR spectra were recorded at 25 °C in CD₃CN on a Bruker Avance III 400 spectrometer operating at 400.17 (¹H), 128.39 (¹¹B), 100.62 (¹³C), 376.45 (¹⁹F), and 71.67 MHz (¹⁹⁹Hg) or on a Bruker Avance DRX-500 spectrometer operating at 500.13 (¹H), 125.76 (¹³C), 160.46 (¹¹B), 470.59 (¹⁹F), and 89.58 MHz (¹⁹⁹Hg). The NMR signals were referenced against TMS (¹H, ¹³C), BF₃·OEt₂ in CD₃CN (¹¹B), CFCl₃ (¹⁹F), and Ph₂Hg in DMSO-*d*₆ (1 mol L⁻¹) (¹⁹⁹Hg, $\delta(^{199}\text{Hg}) = -1187$ ppm;²⁶ Me₂Hg, $\delta(^{199}\text{Hg}) = 0$ ppm) as external standards. Elemental analyses (C, H, N) were performed with a Euro EA3000 instrument (HEKA-Tech, Germany). Thermoanalytical measurements were made with a Mettler Toledo DSC 30 instrument. Temperature and sensitivity calibrations in the temperature range of 25–600 °C were carried out on samples of Ga, In, Pb, Sn, and Zn. About 5–10 mg of the solid samples was weighed and contained in sealed aluminum crucibles, and the studies were performed with a heating rate of 5 K min⁻¹. Throughout this process, the furnace was flushed with dry nitrogen.

Chemicals. All standard chemicals were obtained from commercial sources. Cesium carba-*closo*-dodecaborate was synthesized from $[\text{Me}_3\text{NH}][\text{nido-B}_{11}\text{H}_{14}]^{27}$ following an improved protocol²⁸ of a literature procedure.²⁹ The salts $\text{Cs}[1\text{-H-closo-1-CB}_{11}\text{Cl}_{11}]^{30}$ $\text{Cs}[1\text{-H-closo-1-CB}_{11}\text{Br}_{11}]^{30}$ and $\text{Cs}[1\text{-H-closo-1-CB}_{11}\text{I}_{11}]^{30}$ were prepared similar to published procedures starting from $\text{Cs}[\text{closo-1-CB}_{11}\text{H}_{12}]$. $[\text{Et}_4\text{N}]_2[\text{Hg}(\text{closo-1-CB}_{11}\text{F}_{11})_2]$ and $[\text{Et}_4\text{N}][\text{PhHg}(\text{closo-1-CB}_{11}\text{F}_{11})]$ were synthesized as described recently.¹¹ The synthesis of $\text{C}_6\text{F}_5\text{HgCl}$ is described in the Supporting Information.

Mass Spectrometry. ESI-MS measurements were performed on a Bruker Esquire-LC ion trap mass spectrometer (Bruker Daltonik,

Bremen, Germany). Samples were dissolved in acetonitrile (LCMS grade; VWR, Darmstadt, Germany) at concentrations of approximately 10^{-5} – 10^{-6} mol L⁻¹ and injected into the mass spectrometer via a syringe pump at a flow rate of 3 μ L min⁻¹. Spectra were recorded in the negative ion mode for 3–5 min and averaged.

Collision-induced dissociation (CID) was induced in an ion trap. Ions with a defined m/z value are isolated and specifically activated by collisions with the background gas (mainly He, and some N₂ and H₂O) in the ion trap. The collision is induced by applying an adjustable ac voltage to the ion trap end caps. The resulting mass spectrum shows only the reaction products of the isolated and activated ions. All fragmentation steps were verified by tandem-MS experiments.

Matrix-assisted laser desorption/ionization (MALDI) mass spectra in the negative-ion mode were recorded on a Bruker Ultraflex TOF spectrometer.

Single-Crystal X-ray Diffraction. Colorless crystals of Cs₂·1·2Et₂O suitable for X-ray diffraction studies were grown from a mixture of diethyl ether and acetone (1:1 v/v) by slow evaporation of the solvents. Similarly, crystals of Cs₂·3·MeCN and Cs₂·4·4Me₂CO were obtained from acetonitrile and acetone, respectively. Slow uptake of diethyl ether into a solution of [Et₄N]·6·0.5Me₂CO in acetone resulted in colorless crystals, and crystals of Cs9 were grown from acetone by slow evaporation of the solvent. A crystal of Cs₂·1·2Et₂O, Cs₂·3·MeCN, and [Et₄N]·6·0.5Me₂CO was investigated with an imaging plate diffraction system (IPDS, Stoe & Cie), and a crystal of Cs₂·4·4Me₂CO and Cs9 was studied using a Stoe STADI CCD diffractometer using Mo K α radiation (λ = 0.71073 Å). Numerical absorption corrections³¹ based on indexed crystal faces were applied to the data of all compounds after optimization of the crystal shape.³² All structures were solved by direct methods,^{33,34} and refinement is based on full-matrix least-squares calculations on F^2 .^{34,35}

The positions of most of the hydrogen atoms in the crystal structures were located via ΔF syntheses. The only exceptions are those of the hydrogen atoms of the acetone molecules in [Et₄N]·6·0.5Me₂CO and Cs₂·4·4Me₂CO as well as of the disordered solvent molecules Et₂O and acetonitrile in Cs₂·1·2Et₂O and Cs₂·3·MeCN, respectively. All non-hydrogen atoms were refined anisotropically. Because of the disorder of Et₂O and MeCN in the structures of the cesium salts of 1 and 3, distance and similarity restraints for the anisotropic displacement parameters of these solvent molecules were necessary. In the structures of [Et₄N]·6·0.5Me₂CO and Cs9, similarity restraints for the anisotropic displacement parameters of some of the cluster carbon and boron atoms were introduced to achieve a stable refinement. All hydrogen atoms were refined using idealized bond lengths as well as angles, and their isotropic displacement parameters were kept equal to 120% of the respective parent carbon or boron atom except for the hydrogen atoms of the CH₃ groups, whose isotropic displacement parameters were set to 150% of the respective parent carbon atom.

Molecular structure diagrams were drawn with the program Diamond 3.2g.³⁶ Experimental details, crystal data, and CCDC numbers are collected in Table 5. The supplementary crystallographic data for this publication are found in the Supporting Information or can be obtained free of charge from the Cambridge Crystallographic Data Centre via www.ccdc.cam.ac.uk/data_request/cif.

Quantum Chemical Calculations. Density functional calculations (DFT)³⁷ using the hybrid functional B3LYP³⁸ and Pople-type basis sets 6-311++G(d,p)³⁹ for all atoms except for iodine were performed with the Gaussian 03 program suite.⁴⁰ For iodine and mercury, pseudopotentials were used as implemented in the SDD basis sets in the Gaussian 03 program suite.⁴⁰ DFT calculations with the LDA functionals slater-dirac-exchange,⁴¹ and S-VWN,^{41,42} as well as ab initio calculations employing second-order Møller–Plesset (MP2) perturbation theory⁴³ were done with the Turbomole V6.0 program package.⁴⁴ The resolution-of-the-identity approximation was used for S-VWN and slater-dirac-exchange ((RI)-DFT⁴⁵) as well as MP2 calculations ((RI)-CC2⁴⁶). def2-TZVPP basis sets were employed for (RI)-S-VWN and (RI)-slater-dirac-exchange, and def2-SVP basis sets for (RI)-MP2 calculations.⁴⁷ For iodine and mercury, a relativistic

small-core potential was used (def2-ecp⁴⁷). All structures of the DFT calculations represent true minima with no imaginary frequency on the respective hypersurface. For the (RI)-MP2 calculations, no frequency analyses were performed.

Synthesis of [Et₄N]₂[Hg(closo-1-CB₁₁H₁₁)₂] ([Et₄N]₂1). A 70 mL glass finger equipped with a valve with a PTFE stem (Young, London), fitted with a PTFE-coated magnetic stirring bar, was charged with Cs[1-H-closo-1-CB₁₁H₁₁] (300 mg, 1.10 mmol) and tetrahydrofuran (15 mL). After addition of a solution of ⁿBuLi in hexane (0.68 mL, 1.6 mol L⁻¹, 1.10 mmol) at 0 °C, the reaction mixture was warmed to room temperature and stirred for 1 h. A solution of HgCl₂ (152 mg, 0.55 mmol) in THF (15 mL) was added, and the resulting mixture was stirred for further 2 h. The reaction mixture was poured into water (50 mL), and the THF was removed using a rotary evaporator. An aqueous solution of [Et₄N]Br (1.50 g, 7.14 mmol, 10 mL) was added slowly, resulting in the immediate formation of a white precipitate. This solid was filtered off and dried in a vacuum. The crude product, which contained a small amount of [Et₄N][1-H-closo-1-CB₁₁H₁₁] as an impurity, was dissolved in acetone (10 mL), filtered, precipitated by the addition of diethyl ether (50 mL), and dried in a vacuum to yield pure [Et₄N]₂1. Yield: 286 mg (0.38 mmol, 70%). ¹H{¹¹B} NMR (CD₃CN, δ ppm): 1.51 (s, 10H, BH7–11), 1.50 (s, 10H, ³J(¹⁹⁹Hg, ¹H) = 61.6 Hz, BH2–6), 1.17 (s, 2H, BH12). ¹³C{¹H} NMR (CD₃CN, δ ppm): 81.9 (s, ¹J(¹⁹⁹Hg, ¹³C) = 1250 Hz, C_{cluster}). ¹¹B NMR (CD₃CN, δ ppm): -4.9 (d, 2B, ¹J(¹¹B, ¹H) = 132 Hz, B12), -11.8 (d, 10B, ¹J(¹¹B, ¹H) = 136 Hz, B7–11), -14.2 (d, 10B, ¹J(¹¹B, ¹H) = 148 Hz, B2–6). (-)-MALDI-MS m/z (isotopic abundance > 60) calcd for 1 ([C₂H₂₂B₂₂Hg]⁻): 483(69), 484(77), 485(89), 486(100), 487(85). Found: 483(71), 484(79), 485(90), 486(100), 487(84). Anal. Calcd for C₁₈H₆₂B₂₂HgN₂: C, 29.01; H, 8.39; N, 3.76. Found: C, 29.24; H, 8.42; N, 3.76.

[Et₄N]₂[Hg(closo-1-¹³CB₁₁H₁₁)₂]. The ¹³C-labeled compound was synthesized as described for the nonisotopically enriched compounds. ¹⁹⁹Hg{¹H} NMR (CD₃CN, δ ppm): -1018 (s, ¹J(¹⁹⁹Hg, ¹³C) = 1264 Hz).

Preparation of Cs₂[Hg(closo-1-CB₁₁H₁₁)₂] (Cs₂1). In a 250 mL Erlenmeyer flask, [Et₄N]₂1 (160 mg, 0.21 mmol) was suspended in 10 mL of hydrochloric acid (10% v/v), and 100 mL of diethyl ether was added. The mixture was stirred until all solid material dissolved. The ether layer was separated, and the aqueous phase was extracted two more times with Et₂O (2 \times 50 mL). The combined ether solutions that contain dianion 1 and H⁺(solv) as the counteranion were dried with MgSO₄ and filtered, and the volume of the solution was reduced to approximately 20 mL. The resulting mixture was treated with a solution of CsCl (200 mg, 1.19 mmol) in water (5 mL). Ether and water were removed under reduced pressure, and the colorless solid residue was extracted with a total of 60 mL of acetone. The acetone was evaporated, and the semisolid residue was treated with 100 mL of CHCl₃. The mixture was stored in a refrigerator for 2 h. The white solid was isolated by filtration. Yield: 134 mg (0.18 mmol, 85%). Anal. Calcd for C₂H₂₂B₂₂Cs₂Hg: C, 3.20; H, 2.95. Found: C, 3.35; H, 2.88.

Synthesis of Cs₂[Hg(closo-1-CB₁₁Cl₁₁)₂] (Cs₂3) and [Et₄N]₂[Hg(closo-1-CB₁₁Cl₁₁)₂] ([Et₄N]₂3) Method A. The preparation was performed as described for [Et₄N]₂1 starting from Cs[1-H-closo-1-CB₁₁Cl₁₁] (500 mg, 0.76 mmol) and HgCl₂ (104 mg, 0.38 mmol) except for the isolation of the salt(s). The crude product was dissolved in water (25 mL), and the addition of an aqueous solution of CsCl (2 g, 11.9 mmol, 10 mL) resulted in the formation of Cs₂3. After filtration, the crude Cs₂3 was dissolved in acetone (10 mL) and filtered, and after removal of most of the acetone, pure Cs₂3 was obtained as a white solid by the addition of chloroform. Yield: 316 mg (0.21 mmol, 55%). The remaining aqueous solution after the precipitation of the crude cesium salt was diluted with water (25 mL), and slow addition of a solution of [Et₄N]Br (1.50 g, 7.14 mmol) in water (30 mL) resulted in the formation of a white solid that was contaminated with a small amount of [Et₄N][1-H-closo-1-CB₁₁Cl₁₁]. Pure [Et₄N]₂3 was obtained via recrystallization from acetone by slow uptake of Et₂O vapor. Yield: 206 mg (0.14 mmol, 16%). NMR data for anion 3: ¹³C{¹H} NMR (CD₃CN, δ ppm): 80.1 (s, ¹J(¹⁹⁹Hg, ¹³C) = 1800 Hz, C_{cluster}). ¹¹B NMR (CD₃CN, δ ppm): -3.0 (s, 2B, B12),

−8.9 (s, 10B, B7–11), −11.4 (s, 10B, B2–6). $^{199}\text{Hg}\{^1\text{H}\}$ NMR (CD_3CN , δ ppm): −1340 (s). (−)-MALDI-MS m/z (isotopic abundance > 60) calcd for **3** ($[\text{C}_2\text{B}_{22}\text{Cl}_{22}\text{Hg}]^-$): 1497(61), 1499(81), 1501(85), 1502(81), 1503(100), 1504(71), 1505(84). Found: 1497(65), 1499(80), 1501(80), 1502(78), 1503(100), 1504(75), 1505(86). $\text{Cs}_3\text{3}$: Anal. Calcd for $\text{C}_2\text{B}_{22}\text{Cl}_{22}\text{Cs}_2\text{Hg}$: C, 1.59. Found: C, 1.51. $[\text{Et}_4\text{N}]_2\text{3}$: Anal. Calcd for $\text{C}_{18}\text{H}_{40}\text{B}_{22}\text{Cl}_{22}\text{HgN}_2$: C, 14.39; H, 2.68; N, 1.86. Found: C, 15.06; H, 3.12; N, 1.51.

Synthesis of $\text{Cs}_2[\text{Hg}(\text{closo-1-CB}_{11}\text{Cl}_{11})_2]$ (Cs₂3**). Method B.** $\text{Cs}[\text{1-H-closo-1-CB}_{11}\text{Cl}_{11}]$ (260 mg, 0.4 mmol) and 5 equiv of KOH were dissolved in methanol (10 mL), and subsequently, HgCl_2 (54 mg, 0.2 mmol) was added to the clear solution. The reaction mixture was refluxed for 12 h. After cooling to room temperature, deionized water (50 mL) was added and most of the methanol was removed at a rotary evaporator. Dropwise addition of a solution of CsCl (2.00 g, 11.88 mmol) in water (10 mL) resulted in the precipitation of pure $\text{Cs}_2\text{3}$ as a colorless solid. Yield: 226 mg (0.15 mmol, 76%).

Preparation of $\text{Cs}_2[\text{Hg}(\text{closo-1-CB}_{11}\text{Br}_{11})_2]$ (Cs₂4**).** The synthesis of $\text{Cs}_2\text{4}$ was accomplished by both methods described for the preparation of $\text{Cs}_2\text{3}$.

Method A. $\text{Cs}[\text{1-H-closo-1-CB}_{11}\text{Br}_{11}]$ (300 mg, 0.26 mmol) was treated with $^n\text{BuLi}$ in hexane (0.18 mL, 1.6 mol L^{-1} , 0.28 mmol) at 0 °C, followed by the addition of HgCl_2 (35 mg, 0.13 mmol). Yield: 270 mg (0.11 mmol, 83%).

Method B. $\text{Cs}[\text{1-H-closo-1-CB}_{11}\text{Br}_{11}]$ (550 mg, 0.48 mmol) was reacted with HgCl_2 (65 mg, 0.24 mmol) in basic methanol. Yield: 507 mg (0.20 mmol, 85%). $^{13}\text{C}\{^1\text{H}\}$ NMR (CD_3CN , δ ppm): 85.7 (s, $^1\text{J}(^{199}\text{Hg},^{13}\text{C}) = 1930 \text{ Hz}$, $\text{C}_{\text{cluster}}$). ^{11}B NMR (CD_3CN , δ ppm): −3.8 (s, 2B, B12), −9.2 (s, 10B, B7–11), −11.6 (s, 10B, B2–6). ^{199}Hg NMR (CD_3CN , δ ppm): −1311 (s). (−)-MALDI-MS m/z (isotopic abundance > 60) calcd for **4** ($[\text{C}_2\text{B}_{22}\text{Br}_{22}\text{Hg}]^-$): 2216(65), 2217(84), 2218(84), 2219(95), 2220(98), 2221(90), 2222(100), 2223(84), 2224(76), 2225(68), 2226(66). Found: 2216(60), 2217(82), 2218(80), 2219(95), 2220(95), 2221(86), 2222(100), 2223(89), 2224(80), 2225(75), 2226(69). Anal. Calcd for $\text{C}_2\text{B}_{22}\text{Br}_{22}\text{Cs}_2\text{Hg}$: C, 0.97. Found: C, 1.35.

Preparation of $[\text{Et}_4\text{N}][\text{PhHg}(\text{closo-1-}^{13}\text{CB}_{11}\text{H}_{11})]$ ([Et₄N]6**).** A 70 mL glass finger equipped with a valve with a PTFE stem (Young, London), fitted with a PTFE-coated magnetic stirring bar, was charged with $\text{Cs}[\text{1-H-closo-1-}^{13}\text{CB}_{11}\text{H}_{11}]$ (100 mg, 0.36 mmol) and tetrahydrofuran (20 mL). After addition of a solution of $^n\text{BuLi}$ in hexane (0.25 mL, 1.6 mol L^{-1} , 0.40 mmol) at 0 °C, the reaction mixture was warmed to room temperature and stirred for 1 h. A solution of PhHgCl (126 mg, 0.40 mmol) in THF (15 mL) was added, and the resulting mixture was stirred for a further 2 h. The reaction mixture was poured into water (50 mL), the THF was removed using a rotary evaporator, and the aqueous phase was filtered. A solution of $[\text{Et}_4\text{N}]\text{Br}$ (1.50 g, 7.14 mmol) in H_2O (30 mL) was added slowly under stirring. The white precipitate that had formed was isolated by filtration. The crude product that contained a small amount of $\text{Cs}[\text{1-H-closo-1-}^{13}\text{CB}_{11}\text{H}_{11}]$ was dried in a vacuum and dissolved in acetonitrile, and the solution was filtered. The volume of the clear acetonitrile solution was reduced to approximately 5 mL, and addition of diethyl ether (100 mL) resulted in the precipitation of $[\text{Et}_4\text{N}]\text{6}$ as a white solid, which was filtered off, and dried in a vacuum. Yield: 169 mg (0.31 mmol, 85%). NMR data for anion **6**: $^1\text{H}\{^{11}\text{B}\}$ NMR (CD_3CN , δ ppm): 7.5–7.1 (m, 5H, phenyl), 1.69 (s, 5H, $^3\text{J}(^{199}\text{Hg},^1\text{H}) = 44 \text{ Hz}$, BH2–6), 1.59 (s, 5H, BH7–11), 1.21 (s, 1H, BH12). $^{13}\text{C}\{^1\text{H}\}$ NMR (CD_3CN , δ ppm): 165.8 (d, 1C, $^2\text{J}(^{13}\text{C},^{13}\text{C}) = 37.4 \text{ Hz}$, $^1\text{J}(^{199}\text{Hg},^{13}\text{C}) = 1332 \text{ Hz}$, C_{ipso}), 138.8 (s, 2C, $^2\text{J}(^{199}\text{Hg},^{13}\text{C}) = 92 \text{ Hz}$, C_{ortho}), 129.1 (d, 2C, $^4\text{J}(^{13}\text{C},^{13}\text{C}) = 2.0 \text{ Hz}$, $^3\text{J}(^{199}\text{Hg},^{13}\text{C}) = 112 \text{ Hz}$, C_{meta}), 128.9 (s, 1C, $^4\text{J}(^{199}\text{Hg},^{13}\text{C}) = 19 \text{ Hz}$, C_{para}), 87.3 (s, 1C, $^1\text{J}(^{199}\text{Hg},^{13}\text{C}) = 1150 \text{ Hz}$, $^2\text{J}(^{13}\text{C},^{13}\text{C}) = 37 \text{ Hz}$, $\text{C}_{\text{cluster}}$). ^{11}B NMR (CD_3CN , δ ppm): −5.0 (d, 1B, $^1\text{J}(^{11}\text{B},^1\text{H}) = 133 \text{ Hz}$, B12), −11.5 (d, 5B, $^1\text{J}(^{11}\text{B},^1\text{H}) = 135 \text{ Hz}$, B7–11), −13.8 (d, 5B, $^1\text{J}(^{11}\text{B},^1\text{H}) = 149 \text{ Hz}$, B2–6). $^{199}\text{Hg}\{^1\text{H}\}$ NMR (CD_3CN , δ ppm): −917 (s, $^1\text{J}(^{199}\text{Hg},^{13}\text{C}) = 1139 \text{ Hz}$). (−)-MALDI-MS m/z (isotopic abundance > 60) calcd for **6** ($[\text{C}_7\text{H}_5\text{B}_{11}\text{Hg}]^-$): 419(83), 420(100), 421(100), 422(84). Found: 419(85), 420(97),

421(100), 422(81). Anal. Calcd for $\text{C}_{15}\text{H}_5\text{B}_{11}\text{HgN}$: C, 32.76; H, 6.60; N, 2.55. Found: C, 32.91; H, 6.72; N, 2.35.

Synthesis of $\text{Cs}[\text{PhHg}(\text{closo-1-CB}_{11}\text{Cl}_{11})]$ (Cs8**).** The synthesis of **Cs8** was performed similarly to the preparation of $[\text{Et}_4\text{N}]\text{6}$ starting from $\text{Cs}[\text{1-H-closo-1-CB}_{11}\text{Cl}_{11}]$ (200 mg, 0.38 mmol) and PhHgCl (131 mg, 0.42 mmol). However, a solution of CsCl (2 g, 11.88 mmol) in water (5 mL) was slowly added to an aqueous solution of the crude product, resulting in the precipitation of an off-white solid. Crude **Cs8** was dissolved in acetone and filtered. Chloroform (50 mL) was added, and the acetone was removed at a rotary evaporator. Colorless, pure **Cs8** precipitated from the solution at 5 °C overnight. Yield: 196 mg (0.21 mmol, 55%). $^1\text{H}\{^{11}\text{B}\}$ NMR (CD_3CN , δ ppm): 7.5–7.0 (m, phenyl). $^{13}\text{C}\{^1\text{H}\}$ NMR (CD_3CN , δ ppm): 155.4 (s, 1C, $^1\text{J}(^{199}\text{Hg},^{13}\text{C}) = 1837 \text{ Hz}$, C_{ipso}), 137.3 (s, 2C, $^2\text{J}(^{199}\text{Hg},^{13}\text{C}) = 108 \text{ Hz}$, C_{ortho}), 130.4 (s, 1C, $^4\text{J}(^{199}\text{Hg},^{13}\text{C}) = 28 \text{ Hz}$, C_{para}), 129.9 (s, 2C, $^3\text{J}(^{199}\text{Hg},^{13}\text{C}) = 156 \text{ Hz}$, C_{meta}), 85.2 (s, 1C, $^1\text{J}(^{199}\text{Hg},^{13}\text{C}) = 936 \text{ Hz}$, $\text{C}_{\text{cluster}}$). ^{11}B NMR (CD_3CN , δ ppm): −3.8 (s, 1B, B12), −9.2 (s, 5B, B7–11), −11.6 (s, 5B, B2–6). $^{199}\text{Hg}\{^1\text{H}\}$ NMR (CD_3CN , δ ppm): −1057 (s). (−)-MALDI-MS m/z (isotopic abundance > 60) calcd for **8** ($[\text{C}_7\text{H}_5\text{B}_{11}\text{Cl}_{11}\text{Hg}]^-$): 795(89), 796(92), 797(80), 798(100), 799(65), 800(87). Found: 795(86), 796(95), 797(75), 798(100), 799(69), 800(91). Anal. Calcd for $\text{C}_7\text{H}_5\text{B}_{11}\text{Cl}_{11}\text{CsHg}$: C, 9.03; H, 0.54. Found: C, 9.95; H, 0.57.

Synthesis of $\text{Cs}[\text{PhHg}(\text{closo-1-CB}_{11}\text{Br}_{11})]$ (Cs9**).** **Cs9** was prepared as described for **Cs8** using $\text{Cs}[\text{1-H-closo-1-CB}_{11}\text{Br}_{11}]$ (250 mg, 0.22 mmol) and PhHgCl (75 mg, 0.24 mmol) as starting materials. Yield: 240 mg (0.17 mmol, 76%). $^1\text{H}\{^{11}\text{B}\}$ NMR (CD_3CN , δ ppm): 7.4–7.0 (m, phenyl). $^{13}\text{C}\{^1\text{H}\}$ NMR (CD_3CN , δ ppm): 155.4 (s, 1C, $^1\text{J}(^{199}\text{Hg},^{13}\text{C}) = 1844 \text{ Hz}$, C_{ipso}), 137.2 (s, 2C, $^2\text{J}(^{199}\text{Hg},^{13}\text{C}) = 109 \text{ Hz}$, C_{ortho}), 130.5 (s, 1C, $^4\text{J}(^{199}\text{Hg},^{13}\text{C}) = 28 \text{ Hz}$, C_{para}), 129.9 (s, 2C, $^3\text{J}(^{199}\text{Hg},^{13}\text{C}) = 155 \text{ Hz}$, C_{meta}), 93.0 (s, 1C, $^1\text{J}(^{199}\text{Hg},^{13}\text{C}) = 987 \text{ Hz}$, $\text{C}_{\text{cluster}}$). ^{11}B NMR (CD_3CN , δ ppm): −4.3 (s, 1B, B12), −8.6 (s, 5B, B7–11), −11.8 (s, 5B, B2–6). $^{199}\text{Hg}\{^1\text{H}\}$ NMR (CD_3CN , δ ppm): −1002 (s). (−)-MALDI-MS m/z (isotopic abundance > 60) calcd for **9** ($[\text{C}_7\text{H}_5\text{B}_{11}\text{Br}_{11}\text{Hg}]^-$): 1283(64), 1284(68), 1285(62), 1286(100), 1287(97), 1288(99), 1289(83), 1290(94), 1291(76), 1292(65). Found: 1283(65), 1284(71), 1285(66), 1286(100), 1287(99), 1288(100), 1289(85), 1290(97), 1291(77), 1292(64). Anal. Calcd for $\text{C}_7\text{H}_5\text{B}_{11}\text{Br}_{11}\text{CsHg}$: C, 5.92; H, 0.35. Found: C, 5.85; H, 0.36.

Synthesis of $\text{Cs}[\text{PhHg}(\text{closo-1-CB}_{11}\text{I}_{11})]$ (Cs10**).** In analogy to the synthesis described for **Cs8**, the cesium salt of anion **10** was prepared from $\text{Cs}[\text{1-H-closo-1-CB}_{11}\text{I}_{11}]$ (300 mg, 0.18 mmol) and PhHgCl (63 mg, 0.20 mmol). Yield: 290 mg (0.15 mmol, 83%). $^1\text{H}\{^{11}\text{B}\}$ NMR (CD_3CN , δ ppm): 7.4–7.0 (m, phenyl). $^{13}\text{C}\{^1\text{H}\}$ NMR (CD_3CN , δ ppm): 148.0 (s, 1C, $^1\text{J}(^{199}\text{Hg},^{13}\text{C}) = 1803 \text{ Hz}$, C_{ipso}), 137.3 (s, 2C, $^2\text{J}(^{199}\text{Hg},^{13}\text{C}) = 105 \text{ Hz}$, C_{ortho}), 130.2 (s, 1C, $^4\text{J}(^{199}\text{Hg},^{13}\text{C}) \sim 22 \text{ Hz}$, C_{para}), 129.5 (s, 2C, $^3\text{J}(^{199}\text{Hg},^{13}\text{C}) = 153 \text{ Hz}$, C_{meta}), 103.0 (s, 1C, $^1\text{J}(^{199}\text{Hg},^{13}\text{C}) = 1092 \text{ Hz}$, $\text{C}_{\text{cluster}}$). ^{11}B NMR (CD_3CN , δ ppm): −9.9 (s, 1B, B12), −11.4 (s, 5B, B7–11), −16.5 (s, 5B, B2–6). $^{199}\text{Hg}\{^1\text{H}\}$ NMR (CD_3CN , δ ppm): −865 (s). (−)-MALDI-MS m/z (isotopic abundance > 60) calcd for **10** ($[\text{C}_7\text{H}_5\text{B}_{11}\text{I}_{11}\text{Hg}]^-$): 1804(77), 1805(74), 1806(100), 1807(80). Found: 1804(80), 1805(77), 1806(100), 1807(82). Anal. Calcd for $\text{C}_7\text{H}_5\text{B}_{11}\text{CsHgI}_{11}$: C, 4.34; H, 0.26. Found: C, 4.68; H, 0.38.

Attempted Synthesis of $\text{Cs}[\text{C}_6\text{F}_5\text{Hg}(\text{closo-1-CB}_{11}\text{X}_{11})]$ (X = H, F, Cl, Br, I**).** The reactions were performed similar to the syntheses of the Cs^+ and $[\text{Et}_4\text{N}]^+$ salts of the anions **6** and **8–10**. The solution of $\text{C}_6\text{F}_5\text{HgCl}$ in THF was added either at 0 °C or at −78 °C to a solution of the corresponding Li^+/Cs^+ salt of the carboranyl ligand in THF. The NMR spectroscopic and mass spectrometric ((−)-ESI and (−)-MALDI) analyses showed no differences for the reactions performed at the two different temperatures. According to the ^{11}B and ^{19}F NMR spectroscopic data of the reaction mixtures, the main products (>90%) of the reactions are $\text{Hg}(\text{C}_6\text{F}_5)_2$ and the dianions **1–4** and a complex mixture of $\{\text{closo-1-CB}_{11}\text{I}_{11}\}$ derivatives, which probably contain some carba-closo-dodecaboranyl mercury(II) complexes, in the case of the iodinated carba-closo-dodecaborate cluster, respectively.

■ ASSOCIATED CONTENT

■ Supporting Information

A synthetic procedure for $\text{Hg}(\text{C}_6\text{F}_5)_2$; spectroscopic data for $\text{Hg}(\text{C}_6\text{F}_5)_2$ and $\text{C}_6\text{F}_5\text{HgCl}$; tables containing the energies as well as a table with selected bond lengths calculated for the species discussed in the theoretical sections; figures of the (–)-ESI mass spectra, of the crystal structures of $\text{Cs}_2\cdot 1\cdot 2\text{Et}_2\text{O}$, $\text{Cs}_2\cdot 3\cdot 2\text{MeCN}$, and $\text{Cs}_2\cdot 4\cdot 4\text{Me}_2\text{CO}$, of the calculated structures of the dianions 1–5, and of the ^{11}B NMR spectra of anions 6–10; and CIF files giving details of the X-ray crystallographic analyses and the crystal data. This material is available free of charge via the Internet at <http://pubs.acs.org>.

■ AUTHOR INFORMATION

Corresponding Author

*E-mail: j.warneke@uni-bremen.de (J.W.), maik.finze@uni-wuerzburg.de (M.F.).

■ ACKNOWLEDGMENTS

This work was supported by the Deutsche Forschungsgemeinschaft (FI 1628/2-1). The authors thank Professor W. Frank for generous support and Dr. G. Reiss, Mrs. E. Hammes and Mr. P. Roloff as well as Dr. P. Tommes (all Heinrich-Heine-Universität Düsseldorf), Dr. R. Bertermann (Julius-Maximilians-Universität Würzburg), Dr. Thomas Dülcks, and Dorit Kemken (both Universität Bremen) for technical support and helpful discussions.

■ REFERENCES

- (1) (a) Bresadola, S. In *Metal Interactions with Boron Clusters*; Grimes, R. N., Ed.; Plenum Press: New York, 1982; pp 173–237. (b) Bregadze, V. I. *Chem. Rev.* **1992**, *92*, 209–223.
- (2) (a) Hawthorne, M. F.; Zheng, Z. P. *Acc. Chem. Res.* **1997**, *30*, 267–276. (b) Wedge, T. J.; Hawthorne, M. F. *Coord. Chem. Rev.* **2003**, *240*, 111–128.
- (3) (a) Lee, H.; Knobler, C. B.; Hawthorne, M. F. *Angew. Chem.* **2001**, *113*, 3148–3150; (b) *Angew. Chem., Int. Ed.* **2001**, *40*, 3058–3060. (c) Lee, H.; Knobler, C. B.; Hawthorne, M. F. *J. Am. Chem. Soc.* **2001**, *123*, 8543–8549. (d) Lee, H.; Diaz, M.; Knobler, C. B.; Hawthorne, M. F. *Angew. Chem.* **2000**, *112*, 792–794; (e) *Angew. Chem., Int. Ed.* **2000**, *39*, 776–778. (f) Zheng, Z. P.; Knobler, C. B.; Hawthorne, M. F. *J. Am. Chem. Soc.* **1995**, *117*, 5105–5113.
- (4) Schöberl, U.; Magnera, T. F.; Harrison, R. M.; Fleischer, F.; Pflug, J. L.; Schwab, P. F. H.; Meng, X. S.; Lipiak, D.; Noll, B. C.; Allured, V. S.; Rudalevige, T.; Lee, S.; Michl, J. *J. Am. Chem. Soc.* **1997**, *119*, 3907–3917.
- (5) Taylor, T. J.; Burrell, C. N.; Gabbai, F. P. *Organometallics* **2007**, *26*, 5252–5263.
- (6) Shur, V. B.; Tikhonova, I. A. *Russ. Chem. Bull.* **2003**, *52*, 2539–2554.
- (7) Körbe, S.; Schreiber, P. J.; Michl, J. *Chem. Rev.* **2006**, *106*, 5208–5249.
- (8) Ivanov, S. V.; Rockwell, J. J.; Polyakov, O. G.; Gaudinski, C. M.; Anderson, O. P.; Solntsev, K. A.; Strauss, S. H. *J. Am. Chem. Soc.* **1998**, *120*, 4224–4225.
- (9) Tsang, C.-W.; Yang, Q.; Mak, T. C. W.; Xie, Z. *Appl. Organomet. Chem.* **2003**, *17*, 449–452.
- (10) Finze, M.; Sprenger, J. A. P. *Chem.—Eur. J.* **2009**, *15*, 9918–9927.
- (11) Himmelspach, A.; Zähres, M.; Finze, M. *Inorg. Chem.* **2011**, *50*, 3186–3188.
- (12) (a) Finze, M. *Angew. Chem.* **2007**, *119*, 9036–9039; (b) *Angew. Chem., Int. Ed.* **2007**, *46*, 8880–8882. (c) Finze, M.; Sprenger, J. A. P. *Z. Anorg. Allg. Chem.* **2010**, *636*, 1538–1542.
- (13) Finze, M.; Reiss, G. J.; Zähres, M. *Inorg. Chem.* **2007**, *46*, 9873–9883.
- (14) Sprenger, J. A. P.; Finze, M.; Schaack, B. B. *Dalton Trans.* **2010**, *39*, 2708–2716.
- (15) Strauss, S. H.; Ivanov, S. V.; Lupinetti, A. J. Patent Number WO 98/43983; Colorado State University Research Foundation, 1998.
- (16) Sommerfeld, T.; Bhattarai, B. *Phys. Chem. Chem. Phys.* **2011**, *13*, 18393–18397.
- (17) (a) Koski, W. S.; Kaufman, J. J.; Pachucki, C. F. *J. Am. Chem. Soc.* **1959**, *81*, 1326–1331. (b) Huheey, J. E.; Keiter, E.; Keiter, R. L. *Anorganische Chemie. Prinzipien von Struktur und Reaktivität*, 3rd ed.; de Gruyter: Berlin, 2003.
- (18) Warneke, J.; Dülcks, T.; Knapp, C.; Gabel, D. *Phys. Chem. Chem. Phys.* **2011**, *13*, 5712–5721.
- (19) Warneke, J.; Himmelspach, A.; Finze, M. Unpublished results.
- (20) Canty, A. J.; Deacon, G. B. *Inorg. Chim. Acta* **1980**, *45*, L225–L227.
- (21) Bondi, A. J. *Phys. Chem.* **1964**, *68*, 441–451.
- (22) Kobayashi, Y.; Popov, A. A.; Miller, S. M.; Anderson, O. P.; Strauss, S. H. *Inorg. Chem.* **2007**, *46*, 8505–8507.
- (23) Karakida, K.; Fukuyama, T.; Kuchitsu, K. *Bull. Chem. Soc. Jpn.* **1974**, *47*, 299.
- (24) Benedict, W. S.; Gailar, N.; Plyler, E. K. *J. Chem. Phys.* **1956**, *24*, 1139–1165.
- (25) (a) Ivanov, S. V.; Miller, S. M.; Anderson, O. P.; Solntsev, K. A.; Strauss, S. H. *J. Am. Chem. Soc.* **2003**, *125*, 4694–4695. (b) Avelar, A.; Tham, F. S.; Reed, C. A. *Angew. Chem.* **2009**, *121*, 3543–3545; (c) *Angew. Chem., Int. Ed.* **2009**, *48*, 3491–3493. (d) Kessler, M.; Knapp, C.; Sagawe, V.; Scherer, H.; Uzun, R. *Inorg. Chem.* **2010**, *122*, 5223–5230.
- (26) Sen, M. A.; Wilson, N. K.; Ellis, P. D.; Odom, J. D. *J. Magn. Reson.* **1975**, *19*, 323–336.
- (27) Dunks, G. B.; Barker, K.; Hedaya, E.; Hefner, C.; Palmerordonez, K.; Remec, P. *Inorg. Chem.* **1981**, *20*, 1692–1697.
- (28) (a) Küppers, T.; Bernhardt, E.; Willner, H. *Angew. Chem.* **2007**, *119*, 6462–6465; (b) *Angew. Chem., Int. Ed.* **2007**, *46*, 6346–6349.
- (29) Franken, A.; King, B. T.; Rudolph, J.; Rao, P.; Noll, B. C.; Michl, J. *Collect. Czech. Chem. Commun.* **2001**, *66*, 1238–1249.
- (30) Xie, Z.; Tsang, C.-W.; Sze, E. T.-P.; Yang, Q.; Chan, D. T. W.; Mak, T. C. W. *Inorg. Chem.* **1998**, *37*, 6444–6451.
- (31) X-RED 1.20: *Stoe Data Reduction Program*; STOE & Cie GmbH: Darmstadt, Germany, 2000.
- (32) X-SHAPE 1.06: *Crystal Optimization for Numerical Absorption Correction*; STOE & Cie GmbH: Darmstadt, Germany, 1999.
- (33) Sheldrick, G. M. *SHELXS-97: Program for Crystal Structure Solution*; Universität Göttingen: Göttingen, Germany, 1997.
- (34) Sheldrick, G. M. *Acta Crystallogr.* **2008**, *A64*, 112–122.
- (35) Sheldrick, G. M. *SHELXL-97: Program for Crystal Structure Refinement*; Universität Göttingen: Göttingen, Germany, 1997.
- (36) Brandenburg, K. *Diamond 3.2g*; Crystal Impact GbR: Bonn, Germany, 1999–2011.
- (37) Kohn, W.; Sham, L. J. *Phys. Rev. A* **1965**, *140*, 1133–1138.
- (38) (a) Becke, A. D. *Phys. Rev. A* **1988**, *38*, 3098–3100. (b) Becke, A. D. *J. Chem. Phys.* **1993**, *98*, 5648–5652. (c) Lee, C.; Yang, W.; Parr, R. G. *Phys. Rev. B* **1988**, *37*, 785–789.
- (39) For the basis sets and the corresponding literature, see: <http://www.emsl.pnl.gov/forms/basisform.html>.
- (40) Frisch, M. J.; Trucks, G. W.; Schlegel, H. B.; Scuseria, G. E.; Robb, M. A.; Cheeseman, J. R.; Montgomery, J. A., Jr.; Vreven, T.; Kudin, K. N.; Burant, J. C.; Millam, J. M.; Iyengar, S. S.; Tomasi, J.; Barone, V.; Mennucci, B.; Cossi, M.; Scalmani, G.; Rega, N.; Petersson, G. A.; Nakatsuji, H.; Hada, M.; Ehara, M.; Toyota, K.; Fukuda, R.; Hasegawa, J.; Ishida, M.; Nakajima, T.; Honda, Y.; Kitao, O.; Nakai, H.; Klene, M.; Li, X.; Knox, J. E.; Hratchian, H. P.; Cross, J. B.; Bakken, V.; Adamo, C.; Jaramillo, J.; Gomperts, R.; Stratmann, R. E.; Yazyev, O.; Austin, A. J.; Cammi, R.; Pomelli, C.; Ochterski, J. W.; Ayala, P. Y.; Morokuma, K.; Voth, G. A.; Salvador, P.; Dannenberg, J. J.; Zakrzewski, V. G.; Dapprich, S.; Daniels, A. D.; Strain, M. C.; Farkas, O.; Malick, D. K.; Rabuck, A. D.; Raghavachari, K.; Foresman,

J. B.; Ortiz, J. V.; Cui, Q.; Baboul, A. G.; Clifford, S.; Cioslowski, J.; Stefanov, B. B.; Liu, G.; Liashenko, A.; Piskorz, P.; Komaromi, I.; Martin, R. L.; Fox, D. J.; Keith, T.; Al-Laham, M. A.; Peng, C. Y.; Nanayakkara, A.; Challacombe, M.; Gill, P. M. W.; Johnson, B.; Chen, W.; Wong, M. W.; Gonzalez, C.; Pople, J. A. *Gaussian 03*, revision D.01; Gaussian, Inc.: Wallingford, CT, 2004.

(41) Dirac, P. A. M. *Proc. R. Soc. London, Ser. A* **1929**, *123*, 714–733.
Slater, J. C. *Phys. Rev.* **1951**, *81*, 385–390.

(42) Vosko, S.; Wilk, L.; Nusair, M. *Can. J. Phys.* **1980**, *58*, 1200–1211.

(43) Møller, C.; Plesset, M. S. *Phys. Rev.* **1934**, *46*, 618–622.

(44) (a) *Turbomole V6.0 2009*; a development of University of Karlsruhe and Forschungszentrum Karlsruhe GmbH, 1989–2007, TURBOMOLE GmbH: Karlsruhe, Germany, since 2007. Available from <http://www.turbomole.com>. (b) Ahlrichs, R.; Bär, M.; Häser, M.; Horn, H.; Kölmel, C. *Chem. Phys. Lett.* **1989**, *162*, 165–169.

(45) (a) Eichkorn, K.; Treutler, O.; Öhm, H.; Häser, M.; Ahlrichs, R. *Chem. Phys. Lett.* **1995**, *240*, 283–290. (b) Sierka, M.; Hogekamp, A.; Ahlrichs, R. *J. Chem. Phys.* **2003**, *118*, 9136–9148.

(46) Hättig, C.; Weigend, F. *J. Chem. Phys.* **2000**, *113*, 5154–5161.

(47) The corresponding literature for the basis sets can be found at <ftp://ftp.chemie.uni-karlsruhe.de/pub/basen>.